Journal of Molecular Catalysis A: Chemical 307 (2009) 64–70

Contents lists available at ScienceDirect

Journal of Molecular Catalysis A: Chemical

journal homepage: www.elsevier.com/locate/molcata

The interaction of vanadyl porphyrin with the HY zeolite surface

I.P. Zaragoza[a,*], R. Santamaria[b], R. Salcedo[a]

[a] Departamento de Polímeros, Instituto de Investigaciones en Materiales, Universidad Nacional Autónoma de México, D.F., C.P. 04510, Mexico
[b] Departamento de Física Teórica, Instituto de Física, Universidad Nacional Autónoma de México, D.F., C.P. 04510, Mexico

ARTICLE INFO

Article history:
Received 31 July 2008
Received in revised form 4 March 2009
Accepted 6 March 2009
Available online 20 March 2009

PACS:
31.15.E
68.43.Bc
82.75.Qt
31.15.xv
71.15.Pd

Keywords:
HY zeolite
Vanadyl porphyrin
Zeolite cracking
Born-Oppenheimer molecular dynamics
Density functional theory

ABSTRACT

The interaction of vanadyl porphyrin with the acid sites of the HY zeolite surface is investigated. Structural changes, partial population charges and relative energies induced by the interaction between vanadyl porphyrin and the zeolite surface are estimated with recourse to the Born-Oppenheimer semiclassical molecular dynamics technique in conjunction with density functional theory. An energy optimization process indicates that bond lengths and charge populations of the acid sites are barely distorted when vanadyl porphyrin is adsorbed onto the zeolite surface. At the expense of surmounting a large energy barrier, a dynamic interaction results in the breaking of an OH bond of the surface acid site by the vanadyl porphyrin. Given the amount of energy involved in such a process, the destruction of the catalyst crystal structure by vanadyl porphyrin shows a low probability of occurrence.

1. Introduction

The refining process of the crude oil into gasoline and other useful products requires a large quantity of catalysts. Unfortunately, during this process undesirable reactions between the contaminants carried in the crude oil and the catalysts take place, seriously diminishing the quantity of activated catalysts, with consequent reductions in the production line of gasoline and other byproducts [1]. For instance, it is common to find metals like V, Ni, Fe, S, Cu, etc. capable of interacting with, deactivating and even damaging the catalyst [2]. In particular, there is evidence that vanadium complexes can produce the destruction of the HY zeolite, the main catalyst used in the fluid catalytic cracking (FCC) process [3,4], which in turn renders from a third up to a half of the total gasoline of a refinery [5]. Measurements indicate that about 50% of the catalyst surface area is lost for about 4000 ppm of vanadium [2]. Among the different organometallic contaminants containing vanadium, the best characterized are the vanadium oxide species and the vanadyl porphyrins. The characterization has been carried out by means of X-ray [6,7], high-resolution mass spectroscopy [8], electron spin resonance [9], temperature-programmed reduction [10], and electron paramagnetic resonance [11] techniques.

Several mechanisms have been proposed for the zeolite destruction in the presence of vanadium. For instance, the dehydrogenation products of benzene and olefins are preferentially formed on the vanadium sites, reacting further on the zeolite acid sites, which results in coke formation and the catalyst deactivation [1]. Another mechanism involves the formation of vanadic acid according to the reaction $VO_2{}^+ - (HY\ zeo) + 2H_2O \rightarrow H^+ - (HY\ zeo) + H_3VO_4$, thus destroying the zeolite by hydrolysis of the SiO_2/Al_2O_3 framework [12]. The existence of acidic species different to vanadic acid have been also suggested to be responsible for the catalyst deactivation in the FCC process. The acidic species would come from the SO adsorption on the catalytic surface, reacting with the strong acid sites of the zeolite, leading to the loss of crystallinity [13]. The effect of vanadium in the hydrothermal deactivation of the zeolite with and without the presence of rare earth elements has been also discussed. In particular, a lower zeolite surface area is observed for samples containing Ni and V when compared with samples containing only Ni or only V [3]. It has been observed that vanadium presents different oxidation states in the temperature range [300, 500]°C. However, at temperatures exceeding 500 °C, the V(v)

* Corresponding author.
E-mail addresses: ipzaragoza@iim.unam.mx (I.P. Zaragoza), rso@fisica.unam.mx (R. Santamaria), salcedo@servidor.unam.mx (R. Salcedo).

1381-1169/$ – see front matter © 2009 Elsevier B.V. All rights reserved.
doi:10.1016/j.molcata.2009.03.011

species is highly dispersed and is probably in the form of a framework surface species such as $(Si–O)_3V–O$ [14]. On the other hand, by using thermal techniques and complementing with other spectroscopic analysis, Pompe et al. [15] concluded that vanadium is able to pull out oxygen from the zeolite, thus destroying the catalyst. Clearly, the existence of several detrimental pathways of the HY zeolite points out the complexity in understanding at the molecular level its destruction, together with the role that vanadium compounds play in the zeolite destruction.

The effects of vanadium oxides (such as VO, VO_2, V_2O_3 and V_2O_5) on the internal acid sites of the zeolite have been also investigated at the theoretical level [16]. It is found that the breaking of an OH bond of the acid site, with the hydrogen ion escaping from there, permits the interaction between the vanadium atom of the oxides with the catalytic acid site. The response of the support in this interaction is a non-localized charge redistribution that seems to account for the oxidation of vanadium molecules.

The vanadium oxides are not the unique compounds containing vanadium and capable of permanently damaging the zeolite. For instance, it has been found that the vanadium porphyrins being abundant, can reach the catalyst surface [5] and may reduce the catalytic activity of zeolites [15]. Nevertheless, the large size of the vanadyl porphyrins (compared with the small dimensions of the zeolite pores) prevents the vanadyl porphyrins from penetrating the zeolite. As a consequence, the interaction of vanadyl porphyrin with the zeolite occurs at the zeolite surface. Salcedo et al. [17] have investigated the effects that different lateral chains of vanadyl porphyrinates have in their properties, as well as their solubility in different types of polar solvents. Their results indicate that the reactivity of the complexes is increased with substituents, more strongly polluting the catalyst than the molecule without them.

Since the reaction mechanism between vanadyl porphyrin and the acid sites on the zeolite surface is hard to observe with microscopic detail in the laboratory, the aim of the present work is to find the possible reaction mechanism of vanadyl porphyrin with the HY zeolite. In the first stage, the investigation establishes the adsorption of the organometallic molecule on the catalyst surface. In the second stage, the way in which vanadyl porphyrin is adsorbed onto the zeolite is considered as an indicator of a preferential approach of vanadyl porphyrin towards the zeolite surface. We use the Born-Oppenheimer molecular dynamics method to obtain the trajectory of the vanadium ion in its interaction with the aluminum acid site, when the vanadyl porphyrin molecule is given a large initial momentum. This is a model artifact to overcome the potential energy barrier imposed by the repulsion forces of the interacting compounds, without regard to a physical temperature. Given the large size of the porphyrin, we assume that vanadyl porphyrin pushes waters out of its path, directly impacting over the zeolite surface. In this context, the calculations are performed in the absence of water (our results on the interaction of vanadyl porphyrin with water support to some extent such a hypothesis). The dynamics exhibits a destructive reaction in which the vanadium portion of porphyrin tears the OH bond out of the acid site, producing drastic structural and electron changes of the zeolite surface at the expense of surmounting a large energy barrier. In the final stage, the reaction products consist of a porphyrin whose vanadium atom has captured an OH group of the zeolite, and a locally deformed zeolite without its OH group. Our investigation complements other studies in which small vanadium oxides (like V_2O_5) are able to penetrate the internal structure of the zeolite and, under the appropriate thermodynamic conditions, collapse the zeolite [15].

2. Model

Relevant features of the structure and composition of the HY zeolite are known by means of infrared and mass spectroscopy combined together [18,19]. The zeolite consists of a network of nanopores, through which under appropriate conditions of pressure and temperature, small or linear hydrocarbons may diffuse [20]. Tetrahedral (T) silicons (SiO_4) conform the rings that build the nanopores. It is common to find rings made of 12 T sites, with diameters of approximately 0.8 nm [21]. The Al sites of HY zeolite are commonly identified as the acid sites because it is at these places where a deficiency of electron charge occurs, with the consequent catalysis of hydrocarbons at such places. The acid sites located at the external surfaces of the HY zeolite also react with hydrocarbons, which can be larger than the ones traveling in the nanopores. However, the catalytic sites at the external surface exhibit a great propensity to be neutralized, deactivated or damaged by the contaminants carried in the crude oil like Ni- and V-porphyrins, Ni- and V-naphthenates, etc. [15].

In order to simulate the interaction of an exposed catalytic site with vanadyl porphyrin, we chose a crystallographic portion of the HY zeolite surface reported by Parise et al. [22]. It consists of 16 T sites as depicted in Fig. 1. In four arbitrarily chosen T sites the silicon atom was replaced with aluminum, in such a way that the zeolite composition was $(SiO_4)_{12}$ $(AlO_4)_4$, with a Si:Al ratio of 3, in agreement with experimentally observed and stable Y zeolites [22]. In each oxygen bridge linking the Al and Si atoms, a hydrogen atom was attached to compensate the local charge perturbation produced by the replacement of Si by Al. The terminal oxygens were saturated with hydrogens to avoid possible reactivities attributed to dangling bonds. Since the surface model represents the Y branch that conforms the HY zeolite unit cell, there exists a great probability for vanadyl porphyrin interacting with the zeolite surface, as illustrated in panels (a) and (b) of Fig. 2.

The zeolite surface shall be made to interact with a vanadyl porphyrin, a compound commonly found and isolated from the crude oil [9]. In our simulation, the vanadyl porphyrin corresponds to an oxovanadium porphyrin whose stable molecular structure was determined by X-ray crystallographic experiments reported in Ref. [23] (Fig. 1). In the oxovanadium porphyrin structure, the vanadium atom is coordinated with four nitrogens and one terminal oxygen, in such a way that this part of the structure is shown as a square pyramid [24] (Fig. 2). It is the vanadyl group which presumably causes the lack of planarity. The oxovanadium molecule with lateral aliphatic substituents exhibits terminal methyl groups in the different corners [23] (Figs. 1 and 2). Our vanadyl porphyrin is recognized as deoxophylloerythroetioporphyrin vanadium(IV) in the literature. In principle, the vanadyl compound is bigger than the zeolite surface model. Nevertheless, the catalysis exhibits a highly local character in such compounds making the size difference (whenever the surface model is not that small) of second importance. On the other hand, the vanadyl porphyrin reactivity has been investigated in different solvents with low, medium and high values of the dipole moment [17]. The results show that vanadyl porphyrin with aliphatic substituents is soluble in all these solvents. Still, we are not aware of any work describing from a theoretical perspective the reactivity of vanadyl porphyrin with the HY zeolite surface and, from an experimental perspective, most studies have been concerned with the combined effect and synergy of various primary feed contaminants [25,26].

3. Method

We apply density functional theory (DFT) to investigate the interaction between vanadyl porphyrin and the zeolite surface as it is appropriate to determine structural and electronic property changes of large compounds with relatively high accuracy, at a low computational cost. However, the method requires the proposal of an exchange-correlation energy functional in terms of the electron density, as well as basis sets for the molecular orbital rep-

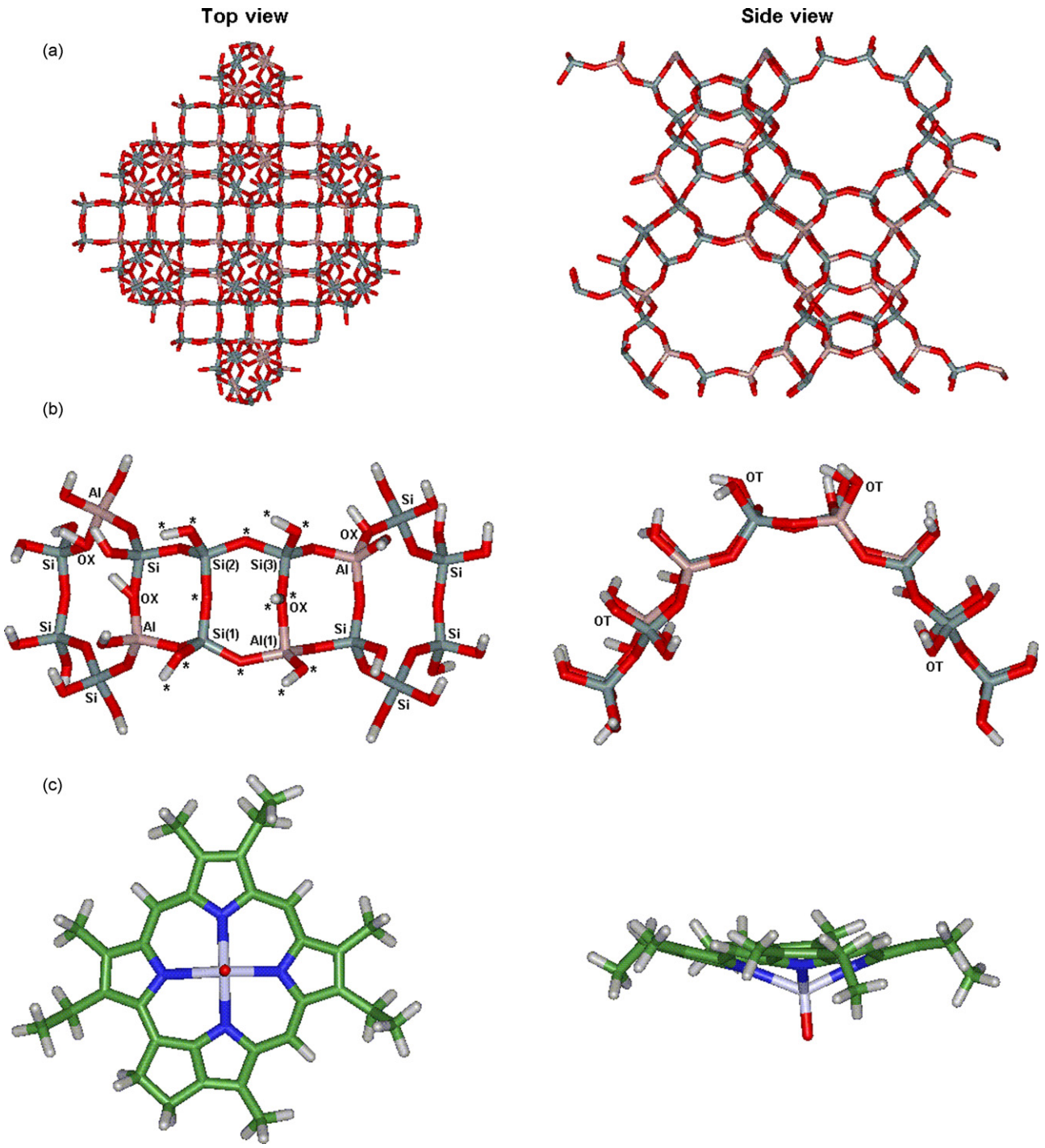

Fig. 1. Top and side views of the HY zeolite together with the vanadyl porphyrin. Panel (a) presents the unit cell, panel (b) the zeolite surface model and panel (c) the vanadyl porphyrin. The zeolite surface model consists of 16 tetrahedral sites. In four of them the Si atom was replaced with the Al atom. Oxygen bridges (OX) linking Al and Si atoms appear with a hydrogen that compensates the local charge neutrality. All terminal oxygens (OT) were saturated with hydrogen (only some of them appear with labels in the figure). Basis sets of the DZVP type were used for all atoms, including these conforming the vanadyl porphyrin, except for the Si and Al atoms of the zeolite lattice that appear without a number, for which a 6–31 G basis set was used. All the vanadyl porphyrin atoms, and Si and Al atoms of the zeolite surface that appear with a number, including their respective oxygens and hydrogens (marked with an asterisk), were allowed to freely move in the optimization process and the molecular dynamics simulation.

resentation. In this regard, the expressions of Becke for exchange [27] and Lee–Yang–Parr for correlation [28] are used to build the exchange-correlation energy functional. This level of theory introduces generalized gradient approximations and is classified within the nonlocal approximations of DFT. When the nonlocal version of DFT is compared with the local approximation of DFT, the nonlocal approach gives an improved prediction of the electronic properties and interaction energies of molecules, due to its higher capacity to explain the anisotropy of the charge distribution. In general, the nonlocal DFT results are found in good agreement with the experimental measurements [29]. With respect to the molecular orbitals, we use atomic basis sets for their description, like the double-zeta valence polarization (DZVP) basis sets. They were specially constructed for use with the DFT approach and exhibit small basis set superposition errors. However, to avoid extensive machine-time usage and other computational bottlenecks attributed to the

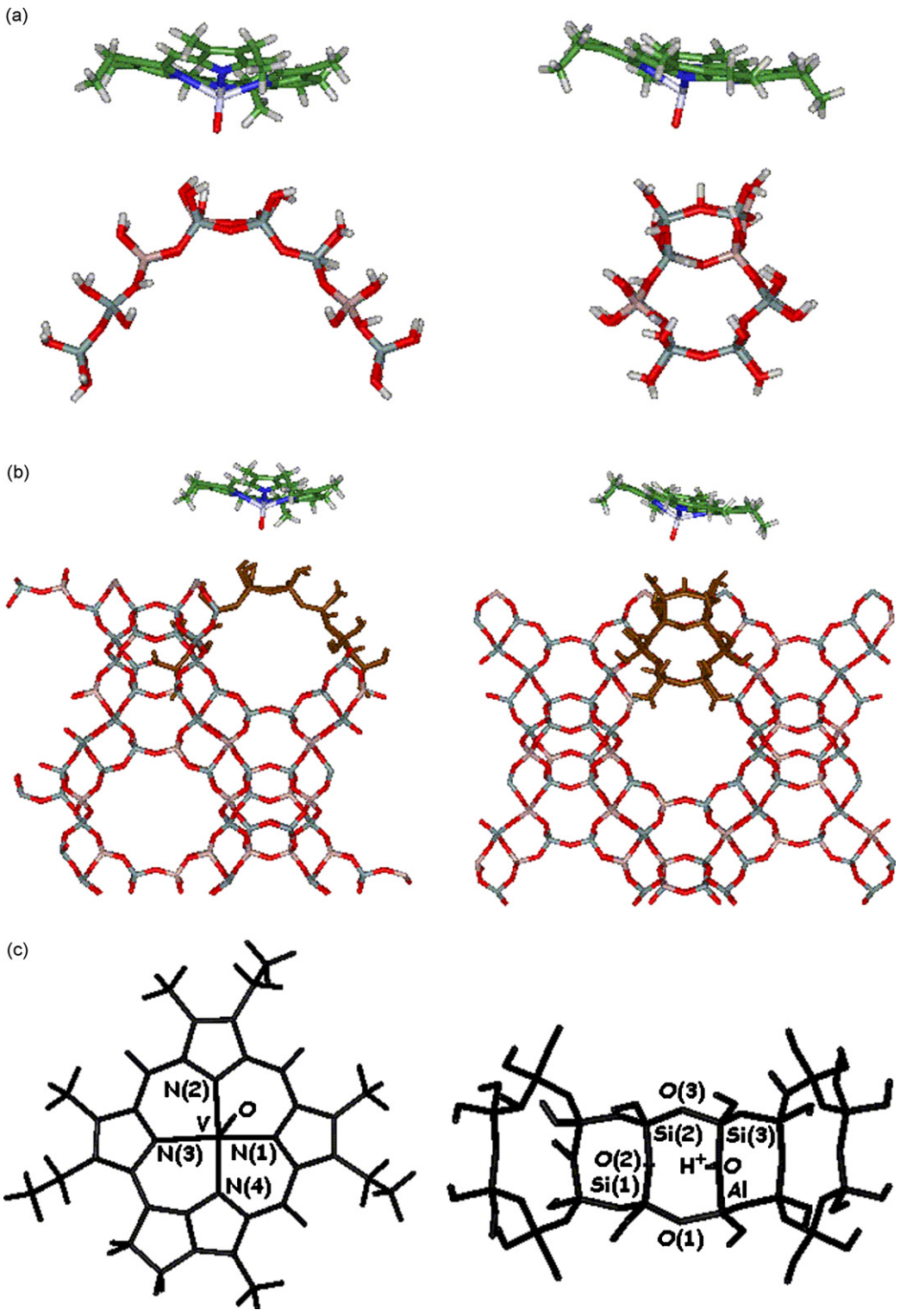

Fig. 2. Lateral views of the zeolite surface and the vanadyl porphyrin. Panel (a) presents the adsorption of vanadyl porphyrin over the zeolite surface as obtained in the energy optimization process. The zeolite surface in this panel is one of many equivalent sections present in panel (b). As an example, the shaded atoms of the zeolite in panel (b) correspond to the zeolite atoms of panel (a). The vanadyl porphyrin is superimposed in panel (b) to have an overview picture of the adsorption process. Panel (c) labels the atoms in the neighborhood of the vanadium atom in the vanadyl porphyrin and these atoms that conform the acid site of the zeolite surface model.

employment of the DZVP basis sets, the 6–31 G basis set is chosen to represent the molecular orbitals of Si and Al atoms not participating in the zeolite catalytic pocket, but forming the zeolite framework (Fig. 1). The 6–31 G basis set should not introduce artificial electronic distortions due to its size. The atoms that do not participate in the zeolite catalytic pocket are assumed to play a less important role in the interaction between vanadyl porphyrin and the catalytic pocket due to their location relatively far away from the surface (Fig. 1).

A charge of +1 for the whole system is considered, and in this case the spin multiplicity is 1 (the reactivity is not biased by such a charge as we shall see later). The scheme used in the optimization tasks

is a quasi-Newton algorithm with line searches and approximate energy Hessian updates, as implemented in the NWChem package [30]. A maximum cartesian step of 0.0015 Bohr and a convergence of 0.0015 Hartree/Bohr in the energy gradients are conveniently chosen. All the vanadyl porphyrin atoms and Si and Al atoms of the zeolite surface facing the porphyrin, including linked oxygens and hydrogens were allowed to freely move in the optimization process (refer to Fig. 1). The remaining atoms were frozen since, under the consideration that the catalysis usually exhibits a local character, they are located far away of the catalytic pocket and hold by a larger framework.

The dynamic aspects of the interaction are simulated with molecular dynamics, particularly using the semiclassical Born-Oppenheimer (BO) approach. In this approach, the electron wave function is computed for (instantaneously) static nuclei, while the nuclear particles are considered classical entities immersed in an average field created by the electrons. The BO scheme applies to cluster calculations, as its present implementation to systems with periodic boundary conditions is still under debate. The time step in the dynamics is 1 fs. The self-consistent approach is considered finished when a convergence of 10^{-5} au in the energy and density are obtained. The atoms allowed to move freely in the molecular dynamics simulation are the same as these in the optimization process. Further details of the method are found in Refs. [29,31]. The computations are performed in a PC cluster using 16 nodes.

4. Results and discussion

The first calculation consists in the energy optimization of vanadyl porphyrin in its interaction with the HY zeolite surface. The vanadyl porphyrin, as observed in Fig. 2, was perpendicularly approached towards the catalytic site of the surface, allowing selected atoms of both entities to relax (those which appear with an asterisk and a number in Fig. 1 of the zeolite surface, and all atoms of vanadyl porphyrin). If we consider that the energy of isolated vanadyl porphyrin (with net charge +1 and when all its atoms have been energetically relaxed) is $E_{VP} = -2500.2559$ au and that the energy of the HY zeolite surface (with net charge 0, under the same relaxation conditions as the vanadyl porphyrin–zeolite surface system) is $E_{SURF} = -7824.4346$ au, then the adsorption energy E_{ads} is estimated from the total energy of the system ($E_{SYS} = -10324.6944$ au) and the energies of the isolated components. In other words:

$$E_{ads} = E_{SYS} - [E_{SURF} + E_{VP}] = -0.0039\,\text{au} \sim -2.4\,\text{kcal/mol}$$

The negative value of the energy certainly indicates an adsorption of porphyrin by the catalytic surface, but it is subtle. Note that in a combined action of sodium, vanadium and steam, an activation energy of 76–79 kcal/mol is registered for the destruction of the Y zeolite [32]. In this regard, the zeolite and vanadyl porphyrin do not really suffer real structural damages in the adsorption process. This is confirmed by the bond lengths and bond angles recorded in Table 1 for the atoms in the neighborhood of vanadium (in the vanadyl porphyrin), and the atoms conforming the acid site of the zeolite surface (refer to panel (c) of Fig. 2) before and after the adsorption takes place.

There are practically no changes in the bond angles of the interacting fragments. A different situation is observed for bond lengths, particularly these of the zeolite which are clearly enlarged. It is the AlO bond length that shows the largest difference as vanadium exerts a strong attraction towards this bond. In order to investigate the net charge fluctuations on atoms, we have computed partial Mulliken charges. Mulliken populations are dependent on basis set, though they simplify the analysis on the redistribution of charges. The partial Mulliken charges reported in Table 2 indicate negligible charge population changes for porphyrin, but noticeable changes for the zeolite atoms. These changes are associated with the presence of vanadium, producing a strong polarization of the zeolite surface atoms. Still, the set of structural and electronic modifications of the catalytic site, produced by the interaction with vanadyl porphyrin, is not considered evidence of a real damage, nor indicative of a disability of that portion of the zeolite surface to carry the catalysis of hydrocarbons. Such results are in agreement with experimental observations [33], which point out an interaction between dispersed metal porphyrins with the zeolitic surface at low porphyrin loadings, and the porphyrins showing slight molecular distortions.

The incapability of porphyrin in the adsorption state to really modify the zeolite structure leads us to apply semiclassical BO molecular dynamics to quantify any possible damage that vanadyl porphyrin may inflict to the zeolite surface. The simulation was started from the conformation obtained in the geometry optimization calculation in the adsorption state. The energy minimum of the system was taken as the zero of the electronic energy in the dynamics. An initial momentum with a preferential direction was imparted to vanadyl porphyrin, in such a way that it could perpendicularly approach the zeolite surface, thus forcing a closer interaction between the zeolite surface and vanadyl porphyrin. The vanadyl porphyrin initial speed (with all its atoms free to move) was 0.002 nm/fs. The kinetic energy is so large that an energy barrier imposed by the repulsive electrostatic forces may be classically

Table 1
Selected bond lengths and angles of vanadyl porphyrin and the HY zeolite surface[a].

Bond lenghts	Isolated	Adsorbed	Bond angles	Isolated	Adsorbed
V–N(1)	2.172	2.167	N(1)–V–O	111	111
V–N(2)	2.226	2.219	N(2)–V–O	114	114
V–N(3)	2.399	2.395	N(3)–V–O	116	116
V–N(4)	2.152	2.150	N(4)–V–O	116	116
V–O	1.592	1.592			
Al–Si(1)	3.196	3.290	Si(1)–Al–Si(2)	43	41
Al–Si(2)	4.814	5.021	Si(2)–Al–Si(3)	39	38
Al–Si(3)	3.704	3.998	Si(1)–Al–Si(3)	82	79
Al–O	2.108	2.411	Al–O–H$^+$	103	104
Si(1)–O(1)	1.651	1.691	O(1)–Si(1)–O(2)	112	112
Si(2)–O(2)	1.661	1.696	O(2)–Si(2)–O(3)	109	111
Si(3)–O(3)	1.698	1.734	O(3)–Si(3)–O	108	105

[a] The results correspond to the porphyrin and HY zeolite surface infinitely separated from each other (isolated column), and to porphyrin adsorbed onto the zeolite surface (adsorbed column). Distances are in Angstroms and angles in degrees. The atom numbers correspond to atom labels given in Fig. 2, panel (c).

Table 2
Partial charges of selected atoms in the porphyrin and the HY zeolite surface[a].

Porphyrin			Zeolite surface		
Atoms	Isolated	Adsorbed	Atoms	Isolated	Adsorbed
V	1.01	1.01	Al	1.03	1.66
N(1)	−0.46	−0.46	O(1)	−0.70	−1.10
N(2)	−0.45	−0.45	O(2)	−0.71	−1.02
N(3)	−0.44	−0.44	O(3)	−0.65	−0.95
N(4)	−0.45	−0.45	O	−0.78	−0.90
O	−0.33	−0.35	H$^+$	0.47	0.46
			Si(1)	1.33	1.89
			Si(2)	1.23	1.77
			Si(3)	1.36	1.81

[a] The results correspond to the porphyrin and HY zeolite surface infinitely separated from each other (isolated column), and porphyrin adsorbed onto the zeolite surface (adsorbed column). Partial charges are computed according to the Mulliken scheme and by subtracting from the atomic number of the element the Mulliken charge, for example, for nitrogen N(2) the atomic number is 7 and the Mulliken charge is 7.45, then the partial charge is 7–7.45 = −0.45. The atom numbers correspond to atom labels given in Fig. 2, panel (c).

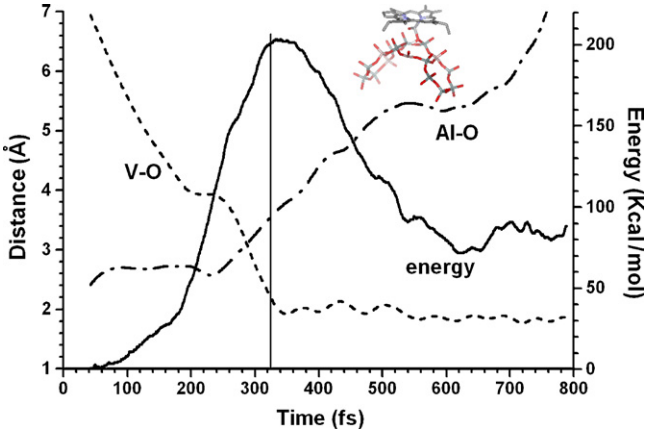

Fig. 3. Variation of selected bond lengths and the electronic energy (including the nucleus–nucleus repulsion) with time. The Al atom is one of the main components of the zeolite acid site and the V atom is the most chemically active element of vanadyl porphyrin. The oxygen is the atom that, in the first stage of the reaction, is linked to the Al atom and, in the second stage of the reaction, is extracted by the V atom. The vertical line divides the two reaction stages. The energy plot is the electronic energy of the vanadyl porphyrin–zeolite system. The zero of the electronic energy corresponds to the energy minimum of the system. The inset presents a frame of the molecular dynamics simulation at the moment in which vanadyl porphyrin attacks the zeolite surface.

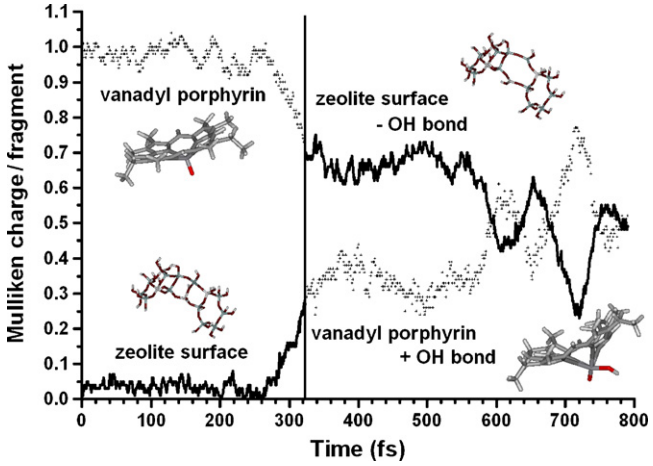

Fig. 4. Variation of Mulliken partial charges of fragments with time. The zeolite surface partial charge is depicted with a continuous line, that of vanadyl porphyrin with cross symbols, that of the zeolite surface without the OH bond is represented by a continuous line and the charge of vanadyl porphyrin plus the OH bond with cross symbols. The vertical line indicates the instant of time when the OH bond is transferred from the zeolite surface to the vanadyl porphyrin. The molecular orientations between the zeolite surfaces, on the one hand, and between the vanadyl porphyrins, on the other, in the insets are approximately the same to observe structural modifications.

overcome. In this regard, the purpose of using a large kinetic energy is to investigate the magnitude of the potential energy barrier, and should not be associated with a physical temperature in this particular situation.

The simulation shows bond-length and bond-angle deformations of the interacting fragments. For instance, Fig. 3 presents the interatomic distances AlO and VO with time changing. The Al atom is one of the four tetrahedral sites facing vanadyl porphyrin, and the oxygen atom of both, AlO and VO, is the bridging oxygen between Al and Si retaining a hydrogen atom (in Fig. 1 Al and O appear with labels Al(1) and OX, this last one with an asterisk). At the initial stage of the dynamics, the AlO bond maintains a stable length, while the VO bond length decreases. Changes in the energy with the time are also plotted in Fig. 3. The energy changes are due to the continuous modification of the atomic interactions during the reaction. The observed energy minimum at the beginning of the simulation is associated with the adsorption of vanadyl porphyrin onto the zeolite surface. The energy value of the system at this early stage is taken as 0 kcal/mol. As the vanadyl porphyrin approaches the zeolite surface, the energy of the system gradually increases; there is an interval of time when the energy increase is almost linear, due to the lack of stability of the AlO bond despite the stability of the VO bond. As the reaction evolves we find an energy barrier whose maximum value is 198 kcal/mol. This takes place when the OH bond is transferred from the zeolite surface to the vanadyl porphyrin. If the energy barriers are associated with a statistical probability of occurrence of the reaction, then the destruction of the zeolite by the vanadyl porphyrin seems to be of low probability, but without meaning that the reaction lacks importance. After the fragments surmount the electronic energy barrier, due to the sufficient nuclear kinetic energy of the porphyrin, a second minimum is found corresponding to the formation of products. It shows an energy of 64 kcal/mol. In the last stage, the product vanadyl porphyrin plus OH bond is stable. Once the OH bond is abducted by the vanadyl porphyrin, a strong repulsion produces the separation of the vanadyl porphyrin plus OH component from the zeolite surface, generating small fluctuations in the energy of the system. The final result consists of two entities, a vanadyl porphyrin with an added OH bond, and a zeolite surface with the loss of such a bond. The reaction can be abbreviated according to the following molecular balance:

$$[\text{zeolite surface}] + [\text{vanadyl porphyrin}] \rightarrow [\text{zeolite surface} - \text{OH}] + [\text{vanadyl porphyrin} + \text{OH}]$$

Note that a few experiments indicate the abstraction of oxygen by vanadium [12,15]. On the other hand, a charge analysis based on Mulliken populations was performed for the vanadyl porphyrin-zeolite surface system. Fig. 4 shows the time evolution of the Mulliken populations for the reactants and products. The analysis divides the system in fragments; one fragment corresponds to the zeolite and the other to the vanadyl porphyrin before and after the reaction. At the first stage (before the OH bond moves from one fragment to the other), the system exhibits a total charge of +1; it is the zeolite which has charge 0 while the vanadyl porphyrin has a net charge of +1. The plots present little variation because the fragments retain their charge when they are far apart. However, there is a short time interval where a greater variation is observed, corresponding to the modification of bond lengths and an increment of the system energy (refer to Fig. 3, correlated with Fig. 4 through the time interval). The variation achieves a maximum when the OH bond is transferred from the zeolite surface to the vanadyl porphyrin (this particular instant of time is depicted with a vertical line in the graph). A charge analysis of the vanadium atom and the OH bond indicates that the positive charge of vanadium is strong enough to pull the negatively charged oxygen of the OH bond apart. In turn, the oxygen drags the positively charged hydrogen atom. In this short time interval the fragment charges are modified as the HY zeolite has lost an OH bond and the vanadyl porphyrin has accepted it. The net charge of vanadyl porphyrin increases (becomes more negative) while that of the zeolite proportionally decreases (becomes more positive). In the final stage of the dynamics, that is, when the fragments are getting separated, charge fluctuations are still observed, but they are expected to diminish once the products are really far away from each other. The results of the dynamics are clearly different to the results obtained in the optimization process, and indicate that the reactivity of the vanadyl compound with the bridging OH group in the zeolite is not biased by a net charge of +1 on vanadyl. In the experiment [33], the porphyrin is apparently desorbed from the zeolite surface, retaining its metal, as in our case,

and there is no mention of the reaction of the OH bond with the porphyrin group.

Finally, in order to analyze the selectivity of vanadyl porphyrin on OH bonds, an additional simulation is carried out, where a water molecule is made to interact with the porphyrin. The orientational aspects and dynamic conditions are the same as for the interaction of the porphyrin with the zeolite surface. The results point out a strong repulsion between reactants, with the water molecule simply bouncing away from the strong electrostatic field created by the porphyrin. In this regard, the porphyrin exhibits a preference for the OH bond of the zeolite surface, despite similar bonds in water molecules.

5. Conclusions

The interaction of vanadyl porphyrin with the HY zeolite surface was studied at the molecular level by using density functional theory and Born-Oppenheimer molecular dynamics. The zeolite surface is capable of adsorbing the vanadyl porphyrin but, as pointed out by the subtle structural modifications of the fragments, the vanadyl porphyrin is incapable of inflicting real damage to the zeolite. On the other hand, a molecular dynamics simulation indicates the predominant role that the acid sites of the zeolite surface play in the interaction with vanadyl porphyrin. In particular, the vanadium ion of the porphyrin shows a strong interaction with the OH^+ bond of the zeolite, pulling it apart from the zeolitic surface at the expense of surmounting a high energy barrier (of approximately 198 kcal/mol). Based on the charge of atoms and fragments, the interaction is characterized in terms of electrostatic interactions. The vanadyl porphyrin in conjunction with the newly attached bond OH is energetically stable. The porphyrin exhibits a selectivity for OH bonds of the zeolite surface, despite similar bonds in water molecules. The charge and mass transfer from the zeolite surface towards the vanadyl porphyrin is indicative of the first stage in the destruction of the crystal structure of the catalyst. However, due to the large energy barrier to overcome, the reaction shows a low probability of occurrence. Still, more studies are required to completely understand the mechanisms promoting the catalyst collapse in order to prevent important losses in the FCC process.

Acknowledgments

I.P.Z and R.S acknowledge DGSCA-UNAM for CPU time allotment in KanBalam. I.P.Z. thanks IMPULSA-UNAM and DGAPA-PROFIP for a postdoctoral fellowship.

References

[1] H.M.T. Oliveira, M.H. Herbst, H.S. Cerqueira, M.M. Pereira, Appl. Catal. A-292 (2005) 82–89.
[2] R.E. Roncolatto, Y.L. Lam, Braz. J. Chem. Eng. 15 (2) (1998).
[3] A.S. Escobar, M.M. Pereira, R.D.M. Pimenta, L.Y. Lau, H.S. Cerqueira, Appl. Catal. A-286 (2005) 196–201.
[4] L.K. Kurihara, M.L. Occelli, S.L. Suib, in: M.L. Occelli (Ed.), ACS Symp. Ser. 452 (1992) 224.
[5] Tolen S Delbert F., Oil Gas J. March-30 (1981) 90.
[6] S. Shimizu, T. Fukuda, N. Kobayashi, K. Saitoh, Anal. Sci. 21 (2005) x17–x18.
[7] H. Duval, V. Bulach, J. Fischer, R. Weiss, Acta Cryst. C54 (1998) 1781–1784.
[8] R.D. Grigsby, J.B. Green, Energy Fuels 11 (1997) 602–609.
[9] M. Espinosa P., A. Campero, R. Salcedo, Inorg. Chem. 40 (2001) 4543–4549.
[10] M.L. Ferreira, M. Volpe, J. Mol. Catal. A: Chem. 184 (2002) 349–360.
[11] C.L. Barbosa Guedes, E. Di Mauro, V. Antunes, A.S. Mangririch, Mar. Chem. 84 (2003) 105–112.
[12] C.A. Trujillo, U.N. Uribe, P.-P. Knops-Gerrits, A.L.A. Oviedo, P.A. Jacobs, J. Catal. 168 (1997) 1–15.
[13] N.P. Martínez, A.M. Quesada P., Catal. Lett 13 (1992) 383–387.
[14] L. Agasi, F.J. Berry, M. Carbucicchio, J.F. Marco, M. Mortimer, F.F.F. Vetel, J. Mater. Chem. 12 (2002) 3034–3038.
[15] R. Pompe, S. Jaras, N.-G. Vannerberg, Appl. Catal. 13 (1984) 171–179.
[16] M. Arroyo, L.E. Sansores, R. Salcedo, J.A. Montoya, J. Nanosci. Nanotechnol. 8 (2009) 1–8.
[17] R. Salcedo, I.P. Zaragoza, J.M. Martínez-Magadán, I. García-Cruz, J. Mol. Struct. (Theochem.) 626 (2003) 195–201.
[18] M. Niwa, K. Suzuki, K. Isamoto, N. Katada, J. Phys. Chem. B 110 (2006) 264–269.
[19] W.H. Baur, Am. Mineralogist 49 (1964) 697–704.
[20] I.P. Zaragoza, L.A. García-Serrano, R. Santamaria, J. Phys. Chem. B109 (2005) 705–710;
M. Palomino, A. Cantin, A. Corma, S. Leiva, F. Rey, S. Valencia, Chem. Commun. (2007) 1233–1235.
[21] A. Corma, F. Rey, S. Valencia, J.L. Jorda, J. Rius, Nat. Mater. 2 (2003) 493–497.
[22] J.B. Parise, D.R. Corbin, L. Abrams, D.E. Cox, Acta Cryst. C40 (1984) 1493–1497.
[23] M.G.B. Drew, P.C.H. Mitchell, C.E. Scott, Inorg. Chim. Acta 82 (1984) 63–68.
[24] M.K. Cyranski, T.M. Krygowski, M. Wisiorowski, N.J.R. van Eikema Hommes, P. von Rague Schleyer, Angew. Chem Int. Eng. 37 (1998) 177–180.
[25] R.E. Ritter, L. Rheaume, W.A. Welsh, J.S. Magee, Oil Gas J. July-6 (1988) 103.
[26] M. Xu, X. Liu, R.J. Madon, J. Catal 207 (2002) 237–246.
[27] A.D. Becke, Phys. Rev. A38 (1988) 3098–3100.
[28] C. Lee, W. Yang, R.G. Parr, Phys. Rev. B37 (1988) 785–789.
[29] I.P. Zaragoza, R. Santamaria, Mol. Phys. 100 (2002) 3139–3145.
[30] E.J. Bylaska, W.A. de Jong, K. Kowalski, T.P. Straatsma, M. Valiev, D. Wang, E. Apra, T.L. Windus, S. Hirata, M.T. Hackler, Y. Zhao, P.-D. Fan, R.J. Harrison, M. Dupuis, D.M.A. Smith, J. Nieplocha, V. Tipparaju, M. Krishnan, A.A. Auer, M. Nooijen, E. Brown, G. Cisneros, G.I. Fann, H. Fruchtl, J. Garza, K. Hirao, R. Kendall, J.A. Nichols, K. Tsemekhman, K. Wolinski, J. Anchell, D. Bernholdt, P. Borowski, T. Clark, D. Clerc, H. Dachsel, M. Deegan, K. Dyall, D. Elwood, E. Glendening, M. Gutowski, A. Hess, J. Jaffe, B. Johnson, J. Ju, R. Kobayashi, R. Kutteh, Z. Lin, R. Littlefield, X. Long, B. Meng, T. Nakajima, S. Niu, L. Pollack, M. Rosing, G. Sandrone, M. Stave, H. Taylor, G. Thomas, J. van Lenthe, A. Wong, Z. Zhang, NWChem, A Computational Chemistry Package for Parallel ComputersVersion 5. 0, Pacific Northwest National Laboratory, Richland, Washington USA, 2006, 99352-0999.
[31] J.M. Martínez-Magadán, S. Meléndez Mercado, R. Santamaria, Chem. Phys. Chem. 11 (2001) 694–700.
[32] L.A. Pine, J. Catal. 125 (1990) 514–524.
[33] S.A. Roth, L.E. Iton, T.H. Fleisch, B.L. Meyers, C.L. Marshall, W.N. Delgass, J. Catal. 108 (1987) 214–232.